the FEBS Journal

Salt-induced formation of the A-state of ferricytochrome *c* – effect of the anion charge on protein structure

Federica Sinibaldi, Maria C. Piro, Massimo Coletta and Roberto Santucci

Dipartimento di Medicina Sperimentale e Scienze Biochimiche, Università di Roma 'Tor Vergata', Italy

Keywords
A-state; cytochrome *c*; fast kinetics; folding; site-directed mutagenesis

Correspondence
R. Santucci, Dipartimento di Medicina Sperimentale e Scienze Biochimiche, Università di Roma 'Tor Vergata', V. Montpellier 1, 00133 Roma, Italy
Fax: +39 06 72596353
Tel: +39 06 72596364
E-mail: santucci@med.uniroma2.it

(Received 1 August 2006, revised 28 september 2006, accepted 5 October 2006)

doi:10.1111/j.1742-4658.2006.05527.x

Structural information on partially folded forms is important for a deeper understanding of the folding mechanism(s) and the factors affecting protein stabilization. The non-native compact state of equine cytochrome *c* stabilized by salts in an acidic environment (pH 2.0–2.2), called the A-state, is considered a suitable model for the molten globule of cytochrome *c*, as it possesses a native-like α-helix conformation but a fluctuating tertiary structure. In this article, we extend our knowledge on anion-induced protein stabilization by determining the effect of anions carrying a double negative charge; unlike monovalent anions (which are thought to exert an 'ionic atmosphere' effect on the macromolecule), divalent anions are thought to bind to the protein at specific surface sites. Our data indicate that divalent anions, in comparison to monovalent ions, have a greater tendency to stabilize the native-like M–Fe(III)–H coordinated state of the protein. The possibility that divalent anions may bind to the protein at the same sites previously identified for polyvalent anions was evaluated. To investigate this issue, the behavior of the K88E, K88E/T89K and K13N mutants was investigated. The data obtained indicate that the mutated residues, which contribute to form the binding sites of polyanions, are important for stabilization of the native conformation; the mutants investigated, in fact, all show an increased amount of the misligated H–Fe(III)–H state and, with respect to wild-type cytochrome *c*, appear to be less sensitive to the presence of the anion. These residues also modulate the conformation of unfolded cytochrome *c*, influencing its spin state and the coordination to the prosthetic group.

Formation of the unique, native structure of a protein occurs through well-defined folding pathways involving a limited number of intermediate species. In recent years, a large body of kinetic and equilibrium studies has provided extensive information on the folding pathway of proteins and led to the characterization of intermediate states, thus contributing to our understanding of the protein-folding mechanism [1–9].

The non-native compact state of equine cytochrome *c* stabilized by salts in an acidic environment (pH 2.0–2.2), called the A-state, is thought to be a suitable model for the molten globule of cytochrome *c*; it possesses a native-like α-helix conformation but a fluctuating tertiary structure [10–14]. With respect to the native protein, in the A-state some interior hydrophobic residues become exposed to the solvent [15], the W59-one-heme-propionate hydrogen bond is impaired (although the tryptophan remains within a hydrophobic environment) [14], and the heme–polypeptide chain interaction is reduced. Also, the hydrophobic core (which is composed of the two major helices and the heme group) is preserved in the A-state,

Abbreviation
CT, charge transfer.

stabilized by nonbonded interactions [12,16], whereas the loop regions appear to be fluctuating and partly disordered [12]. The A-state is promptly achieved at pH around 2.2 upon addition of a salt to an aqueous HCl solution containing denatured cytochrome *c*; this has been ascribed to a screening action of the anions, which stabilize the compact form by binding to the positively charged groups on the protein surface [11].

Recently, we investigated the role played by monovalent anions in promoting the transition from the acid-denatured protein to the A-state [17,18]. Our results showed that the salt-induced A-state of ferricytochrome *c* is characterized by a variety of high-spin and low-spin states (where 'high' and 'low' stand for the $S = 5/2$ and $S = 1/2$ spin states of the heme iron, respectively) in equilibrium; in particular (at least), two distinct low-spin species, differing in their axial ligation to the metal, coexist in solution: a form with the native M–Fe(III)–H coordination, and a bis-histidine coordinated species. The equilibrium between these two low-spin forms, here indicated as M-Fe (III)-H $\leftrightarrow$ H-Fe(III)-H is strongly influenced by the type of anion in solution [17,18].

Because structural information on partially folded forms is important for a deeper understanding of the folding mechanism(s) and the factors affecting protein stabilization, in this article we extend our knowledge on anion–protein interactions by determining the effect on the protein produced by anions carrying a double negative charge. This is an interesting point to investigate, because, unlike monovalent anions (which are thought to exert an 'ionic atmosphere' effect on the macromolecule), divalent anions (as well as polyvalent groups, such as polyphosphates [19,20]) are supposed to bind to the protein at specific surface sites [21,22].

Results

Horse ferricytochrome *c*

CD measurements

Far-UV CD (200–250 nm) is a probe for the formation of the A-state from acid-denatured cytochrome *c*, as the A-state possesses a native-like α-helix structure [11,17]. Figure 1 shows the gradual recovery of the ordered secondary structure in acid-denatured ferricytochrome *c* upon addition of increasing amounts of sulfate and selenate; the divalent anions stabilize the A-state at significantly lower concentrations than those needed for stabilization by monovalent ions [17]. As shown in Fig. 2, the A-state tertiary conformation is less packed than that of the native form; the protein displays a weaker near-UV CD spectrum (Fig. 2A),

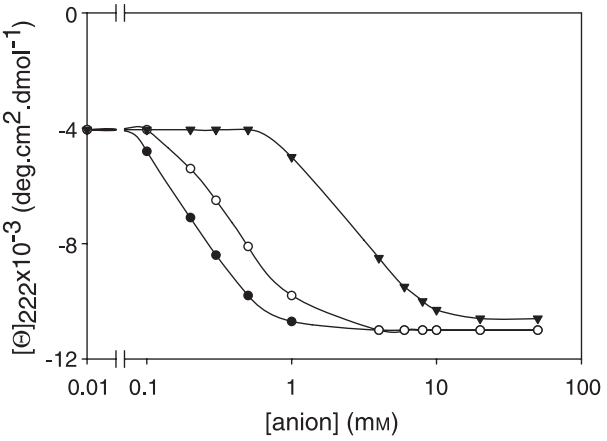

Fig. 1. Sulfate-induced (●) and selenate-induced (○) conformational transition of acid-denatured cytochrome *c* to the A-state, as measured by the ellipticity at 222 nm. Experimental conditions: aqueous HCl, pH 2.2; temperature 25 °C. The transition in perchlorate (▼) is shown for comparison.

consistent with a perturbed W59 microenvironment, and a weaker Soret CD spectrum (Fig. 2B). In this last case, the decreased intensity of the 416 nm Cotton effect is indicative of a perturbed heme pocket region, as the 416 nm dichroic band is considered to be diagnostic for the Met80–Fe(III) coordination in native cytochrome *c* [23,24]). As the M–Fe(III)–H coordinated species alone contributes to the dichroic signal, a significant population of macromolecules is expected to lack M80 coordination to Fe (III) in the A-state (it must be noted, however, that the signal is stronger than that recorded in the presence of monovalent anions [17,18]). The intensity of the 416 nm dichroic band is ~35% that of the native state, consistent with heterogeneity of the A-state. On the basis of earlier data (relative to monovalent anions) [18], a mixture between Met80–Fe(III)–His18 coordinated species and X-Fe-His18 miscoordinated species (where X represents the endogeneous ligand coordinated to the metal in place of Met80) is expected in solution. Under the conditions investigated, a histidine (His26 or His33) is expected to be the best candidate for ligand X (the other likely candidates, i.e. the lysines, are fully protonated at pH 2.2) [18].

The heterogeneous character of the A-state prompted us to investigate the effect of sulfate and selenate on the heme pocket conformation. As shown in Fig. 3, the 416 nm dichroic band gradually increases (towards negative ellipticity values) with anion concentration, up to 4 mM anion; it then remains unchanged (up to 40 mM anion). This behavior markedly differs from that displayed by the protein in the presence of

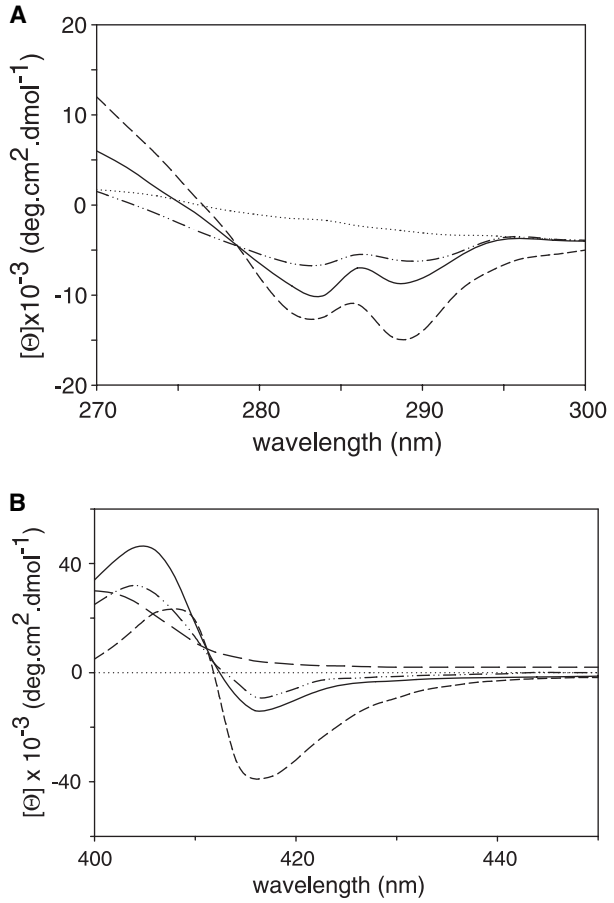

Fig. 2. Near-UV (A) and Soret (B) CD spectra of acid-denatured cytochrome *c* in the presence of 0.02 M sulfate (—) and 0.02 M selenate (— ··— ··). The spectra of the native (-·-·-) and of the denatured (····) protein are shown for comparison. Protein concentration: 10 μM. Other experimental conditions were as described in the legend to Fig. 1.

monovalent anions (the effect of perchlorate is illustrated in Fig. 3 for comparative purposes). The changes in the Cotton effect strength observed at high monovalent anion concentrations have been attributed to a shift of the M-Fe(III)-H ↔ H-Fe(III)-H equilibrium towards formation of the bis-H species [18]. Thus, the data in Fig. 2 indicate that divalent anions have a stronger tendency to stabilize the (native-like) M–Fe(III)–H coordinated form.

Unfolded macromolecules and peptides attain a degree of structure at temperatures lower than room temperature. We have recently shown that the A-state induced by monovalent anions displays a temperature-dependent 416 nm Cotton effect (temperature range: 25 °C to 2 °C) [17]. In the present study, the investigation, extended to divalent anions, confirms that the native M–Fe(III)–H bond (indicative of a more structured conformation) is stabilized by low temperature (data not shown), indicating that protein flexibility hinders methionine coordination to the heme iron [25].

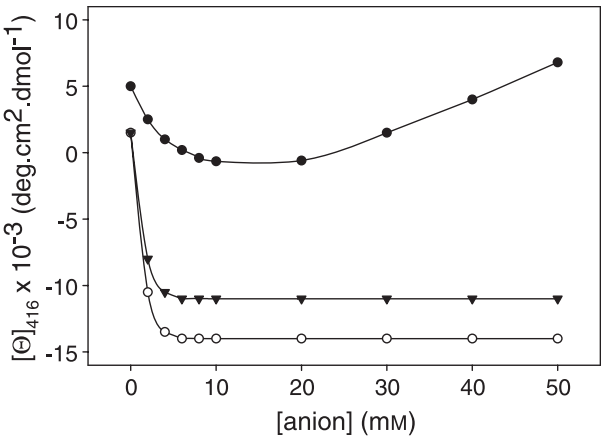

Fig. 3. Effect of sulfate (○) and selenate (▼) concentration on the heme pocket environment [and on the strength of the Met80–Fe(III) axial bond] of the salt-induced A-state of cytochrome *c*, as observed from changes induced in the 416 nm Cotton effect. The effect induced by the monovalent anion perchlorate (●) is reported for comparison. Other experimental conditions were as described in the legend to Fig. 1.

Electronic absorption

The 695 nm absorption band is considered to be diagnostic for the M80–Fe(III) axial bond in native cytochrome *c* [26]. Figure 4 shows the effect of sulfate and selenate on acid-denatured cytochrome *c*, investigated

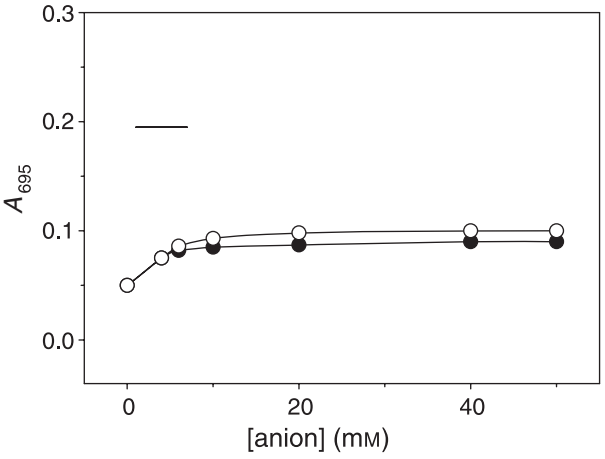

Fig. 4. Absorbance at 695 nm of acid-denatured cytochrome *c* in the presence of increasing sulfate (○) and selenate (●) concentrations. The optical absorbance of native cytochrome *c* (—) at pH 7.0 is shown for comparison. Protein concentration: 0.25 mM. Other experimental conditions were as described in the legend to Fig. 1.

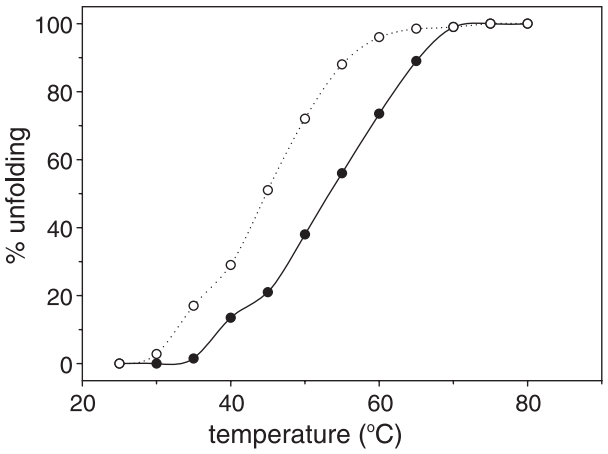

Fig. 5. Thermal stability of the A-state of cytochrome *c* as a function of sulfate concentration. Sulfate concentration: ○, 10 mM; ●, 40 mM. The experimental points refer to ellipticity values at 222 nm. Other experimental conditions were as described in the legend to Fig. 1.

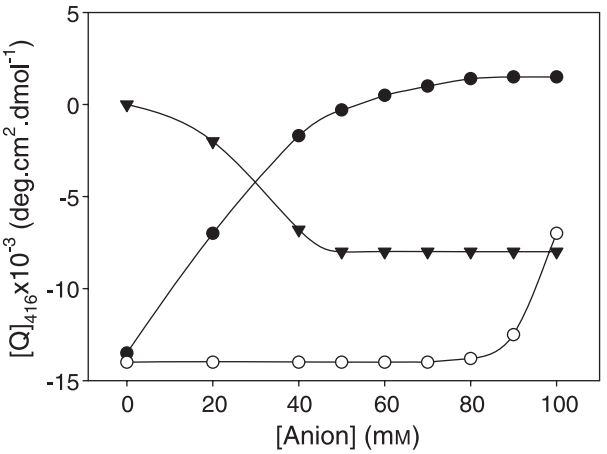

Fig. 6. Effect of perchlorate (●) and chloride (○) concentration on the heme pocket environment of the sulfate-induced A-state of cytochrome *c*, as observed from changes induced in the 416 nm Cotton effect (sulfate concentration: 50 mM). The effect of sulfate (▼) concentration on the perchlorate-induced A-state is also illustrated (perchlorate concentration: 50 mM). Other experimental conditions were as described in the legend to Fig. 1.

by following the changes in the 695 nm absorbance band. It appears clear that both anions favor protein collapse into a compact form, and induce formation of a consistent population of macromolecules ($\sim$ 35% in sulfate, $\sim$28% in selenate) with native M–Fe(III)–H coordination. These data are in excellent agreement with CD measurements and provide independent evidence for heterogeneity of the A-state.

A-state stability

Figure 5 shows the thermal denaturation profiles of the A-state of cytochrome *c*, as obtained from ellipticity values at 222 nm. As previously observed for mononvalent anions [18], the shape of the unfolding profiles features a multiple state transition, as (at least) three distinct thermodynamic states are detected. The profiles clearly show that protein stability strongly depends on anion concentration; this highlights the primary role played by the anion–protein interactions in A-state stabilization.

Competition among anions

To better define the effect produced by monovalent anions on the sulfate-induced A-state of cytochrome *c*, we monitored the changes in the 416 nm Cotton effect induced by increasing amounts of perchlorate and chloride. As shown in Fig. 6, addition of monovalent anions alters the 416 nm dichroic band; this suggests competition between monovalent and divalent anions for binding to the protein. In particular, both perchlorate and Cl^- shift the M-Fe(III)-H $\leftrightarrow$ H-Fe(III)-H equilibrium towards the bis-H species, and destabilize the M–Fe(III)–H coordinated form. The reduced effect of Cl^- reflects the different affinities of the two anions for the protein [11,17].

We also monitored the effect of sulfate on the perchlorate-induced A-state. As shown in Fig. 6, addition of sulfate strengthens the 416 nm dichroic band, which confirms that divalent anions have a greater tendency to stabilize the M80–Fe(III)–H18 coordinated form. On the whole, these data support competitive anion binding to the protein, and the idea that monovalent and divalent anions tend to stabilize differently structured A-states.

Horse ferricytochrome *c* variants

Anions carrying multiple negative charges bind to specific sites of horse cytochrome *c* [19,27]. To determine whether divalent anions bind to the same sites, we introduced some mutations within the site-containing regions of the macromolecule, with the aim of defining the role played by single residues in modulating protein affinity for divalent anions. On the basis of earlier work [19,27], the sites under consideration were: (a) the site encompassing residues K87, K88, and R91, located in the C-terminal α-helix segment, indicated here as site 1; and (b) the site encompassing residues K86, K87, and K13, located at the interface between the N-terminal and the C-terminal α-helices, indicated

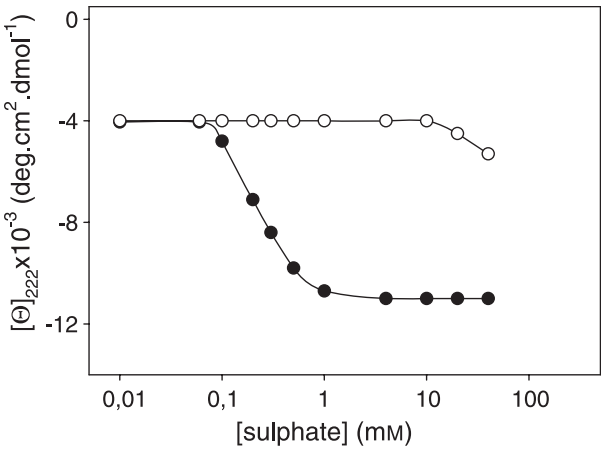

Fig. 7. Sulfate-induced conformational transition of acid-denatured horse ferricytochrome *c* (●) and yeast iso-1-ferricytochrome *c* (○) to the A-state, as measured by the ellipticity at 222 nm. Experimental conditions: aqueous HCl, pH 2.2; temperature 25 °C.

here as site 2. The residues under investigation were substituted with residues located at the same position in yeast iso-1-cytochrome *c*; as illustrated in Fig. 7, horse and yeast cytochrome *c* show very different affinities (considered here as a nonspecific indicator of the binding effect, not as a direct measure of anion binding to the protein) for anions.

CD and absorption measurements

In site 1, the K88E mutation introduces an acidic residue (E88, present in yeast [28]) in place of a lysine, whereas in site 2, the K13N mutation introduces an asparagine in place of a lysine. This provides the opportunity to evaluate the contribution of K88 and K13 to protein stabilization in the reaction with sulfate. The far-UV and Soret CD spectra of the two mutants (not shown) reveal that the two variants and the wild-type protein are equally influenced by sulfate. Similar results were obtained when we investigated the spectroscopic properties of the K88E/T89K double mutant, which, with respect to the K88E mutant, possesses a sequence closer to the corresponding sequence in yeast iso-1-cytochrome *c*. A 40 mM sulfate concentration induced, in all the variants investigated, native-like α-helix content and formation of the 416 nm Cotton effect with a strength comparable (although not identical) to that of the wild-type protein. This excludes the possibility that K88, T89 and K13 modulate horse cytochrome *c* affinity for anions. Also, the mutant's stability is not dissimilar to that of the wild-type protein, as indicated by thermal denaturation studies (data not shown).

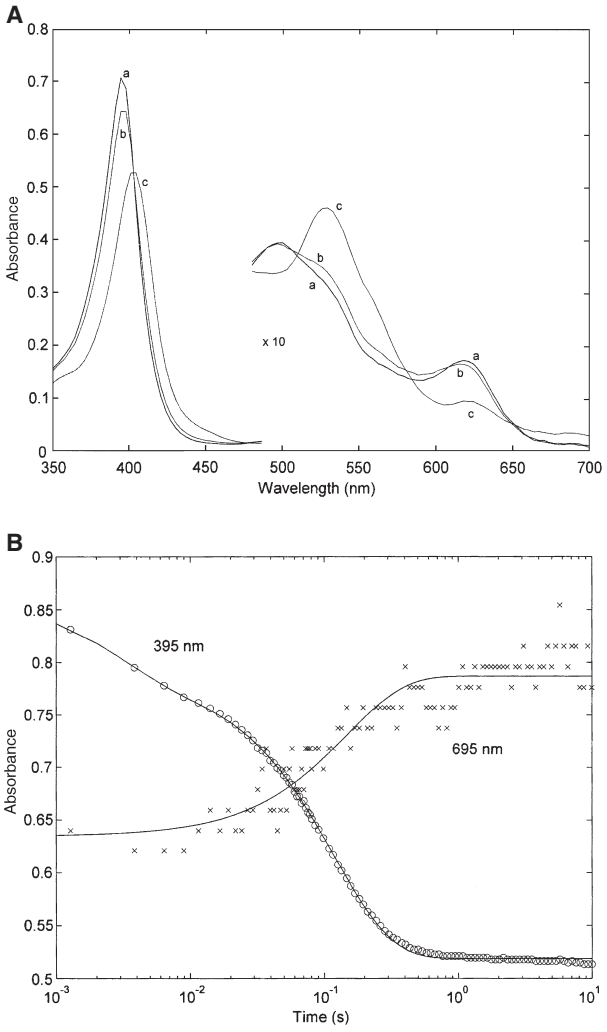

Fig. 8. (A) Absorption spectra of ferricytochrome *c* before (spectrum a) and after 40 ms (spectrum b) and 5 s (spectrum c) of mixing with 40 mM sulfate. Absorption spectra in the visible range are a 10-fold magnification of original spectra. (B) Kinetic progress curves of wild-type cytochrome *c* after mixing with 40 mM sulfate at 395 nm and at 695 nm, as indicated. The progress curve at 695 nm has been magnified in order to compare its signal time evolution with that at 395 nm. The solid lines are the least-squares nonlinear fitting of the kinetic progress curve according to Eqn (1), with $n = 2$ and with the following rate constants: $k_1 = 350 \pm 40$ s^{-1} and $k_2 = 8.4 \pm 0.9$ s^{-1} at 395 nm, and $k = 7.7 \pm 0.7$ s^{-1} at 695 nm.

Fast kinetic measurements

The 350–700 nm absorption spectrum of acid-denatured cytochrome *c* (spectrum a of Fig. 8A) displays an absorption maximum around 395 nm in the Soret region, and a maximum at 497 nm, a shoulder at 528 nm and a charge transfer (CT) at 618 nm in the visible region. The spectral changes detected at pH 2.2

upon mixing acid-denatured cytochrome *c* with sulfate (final anion concentration 40 mM) are shown in Fig. 8B. At 395 nm, the kinetic process appears to be biphasic, characterized by a fast phase ($k_{obs} = 50 \pm 40\ s^{-1}$) and a slow phase ($k_{obs} = 8.4 \pm 0.9\ s^{-1}$). The process is characterized by a red-shift of the Soret band (initially centered at 395 nm) to 402 nm. In the visible region, complex spectral changes are detected; in particular, the fast phase is characterized by a slight increase of the absorbance band centered at 528 nm and by a blue-shift of the CT band from 618 to 616 nm (spectrum b of Fig. 8A). The slow phase is instead characterized by a marked enhancement of the absorbance band centered at 528 nm (at the expense of the 497 nm peak), whereas the CT band decreases in intensity and red-shifts from 616 nm to 623 nm. This is also accompanied by an increase of the 695 nm band (spectrum c of Fig. 8A), with a rate close to that observed for the slow phase at 395 nm (Fig. 8B). Even though variations of the CT 623 nm band may contribute to the absorption change at 695 nm (thus affecting the amplitude change), the major contribution stems from the 695 nm band; therefore, the observed rate can be attributed to formation of the Fe(III)–M80 axial bond, providing strong indication that the slow phase is coupled to formation of the native axial coordination.

The absorption spectra of the K13N and K88E/T89K mutants, shown in Fig. 9A, differ significantly from that of the acid-denatured cytochrome *c*. The Soret absorbance band is red-shifted (more pronounced in the case of the K13N mutant), and the absorbances at 497 and 528 nm, in the visible region, are inverted, whereas the CT band is weakened and red-shifted. This indicates that the mutations introduced into the protein bring about changes at the level of the heme coordination, and suggests that even the pathway from acid-denatured cytochrome *c* to the A-state may be altered. This hypothesis is supported by data obtained from comparison of the kinetic behavior of the mutants with that of the acid-denatured protein in the reaction with sulfate (Fig. 9B). As mentioned above, at 395 nm the (sulfate-induced) refolding kinetics of acid-denatured cytochrome *c* is biphasic (Fig. 8B); also, the K88E/T89K double mutant shows biphasic behavior, but in this case the fast phase is faster and the absorbance change weaker (Fig. 9B). The biphasicity disappears in the case of the K13N mutant, which shows very small absorbance changes. The optical spectra show that the two mutants differ structurally from the wild-type protein not only in the acid-denatured form, but even as the A-state (i.e. after they have reacted with sulfate); this is particularly evident for the K13N mutant (Fig. 9C). The reduced absorbance change observed may indicate that the variants undergo very fast optical (and thus structural) changes within the dead time of the stopped-flow apparatus. In the case of the K13N mutant, this hypothesis finds support from the fact that the absorption spectrum obtained 3 ms after mixing is already different from that recorded before mixing (Fig. 9D). These kinetic differences do not seem to influence the overall sulfate–protein interaction; as indicated by far-UV and Soret CD spectra (not shown), wild-type cytochrome *c* and the mutants all are equally affected by the sulfate. This rules out the hypothesis that K88, T89 and/or K13 may modulate the protein–anion interaction, even though kinetic data clearly indicate that the introduced mutations influence the anion-linked structural changes occurring in the protein. Thus, if the mutated residues seem to exert no relevant effect on protein stability, they play a role in shaping the pathway of the anion-linked conformational changes.

Discussion

Cytochrome *c* is probably the first protein in which a globular state induced by salt at low pH (the so-called A-state) was named a 'molten globule'. Goto *et al.* demonstrated that the conformational transition from acid-unfolded protein to this globular state is mediated by anion binding to the protein, in which the anion charge plays a primary role; the higher the charge, the lower is the anion concentration required to stabilize the A-state [11]. Subsequent studies have shown that the tertiary conformation of the A-state is modulated by the type of monovalent anion added in solution [17]; furthermore, the protein is characterized by multiple equilibrium states between high spin and low spin, and by (at least) two distinct low-spin states [18]. In particular, the equilibrium governing the low-spin population, M-Fe(III)-H $\leftrightarrow$ H-Fe(III)-H, strictly depends on anion size and concentration. The presence of bis-H low-spin species at pH 2.2 may appear to be unusual, because under these conditions histidines are generally protonated (and thus unable to bind the heme iron as strong ligands). However, spectroscopic data probing the existence of the bis-H low-spin states of cytochrome *c* have recently been published [17,18].

The A-state of cytochrome *c* consists of a native-like folded subdomain (the hydrophobic core, formed by the N-terminal and C-terminal helices and the heme group [12,16,18]) and fluctuating, partially disordered loop regions [12]. Its stabilization by monovalent anions has been ascribed to preferential anion binding to

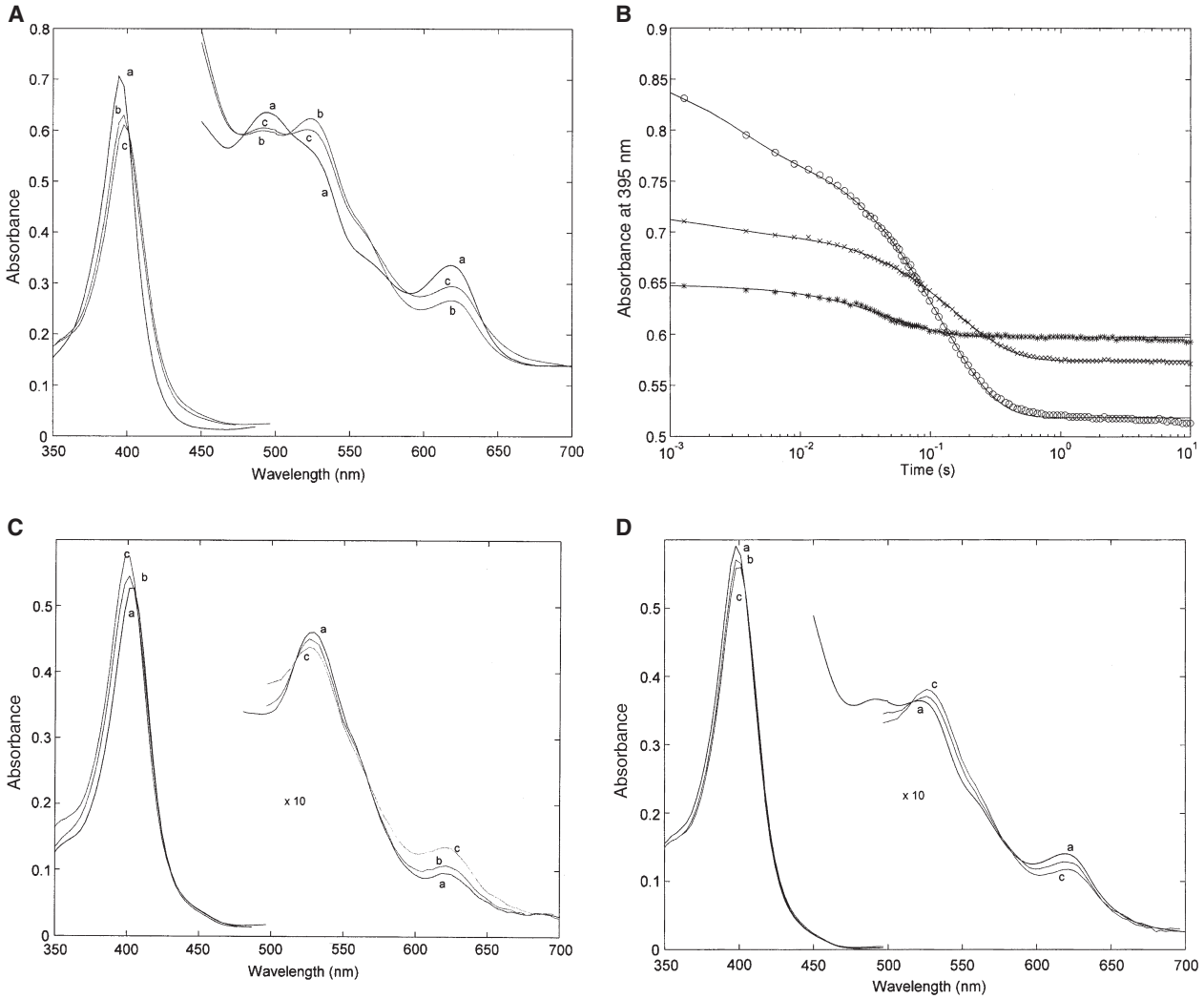

Fig. 9. (A) Static absorption spectra of acid-denatured ferricytochrome *c* (spectrum a), of the K88/T89KE double mutant (spectrum b), and of the K13N mutant (spectrum c). Absorption spectra in the visible range are a 10-fold magnification of original spectra. (B) Kinetic progress curves at 395 nm after mixing 40 mM sulfate with 8 μM cytochrome *c* (o), K88E/T89KE mutant (x), and K13N mutant (*), at 20 °C. Continuous lines are the nonlinear least-squares fitting of data according to Eqn (1), with $n = 2$ for wild-type cytochrome *c* and the K88E mutant, and $n = 1$ for the K13N mutant. The respective rate constants are: $k_1 = 350 \pm 40$ s^{-1} and $k_2 = 8.4 \pm 0.9$ s^{-1} for wild-type cytochrome *c*; $k_1 = 470 \pm 60$ s^{-1} and $k_2 = 7.4 \pm 0.8$ s^{-1} for the K88E/T89KE mutant; and $k_1 = 19.4 \pm 2.3$ s^{-1} for the K13N mutant. (C) Absorption spectra of wild-type cytochrome *c* (spectrum a), of the K88E/T89KE mutant (spectrum b), and of the K13N mutant (spectrum c) after 5 s of mixing with 40 mM sulfate. Absorption spectra in the visible range are a 10-fold magnification of original spectra. (D) Absorption spectra of the acid-denatured K13N mutant (spectrum a), of the K13N mutant after 3 ms of mixing with 40 mM sulfate (spectrum b), and after 5 s of mixing with 40 mM sulfate (spectrum c). Absorption spectra in the visible range are a 10-fold magnification of original spectra. Spectrum b, which is between spectrum a and spectrum c, has not been marked, for the sake of image clarity.

the positively charged clusters located on the protein surface [11]. The distribution of lysines around the heme crevice at the 'front' of the molecule is highly conserved in eukaryotic *c* class cytochromes [27]; anions exert a strong influence on the lysine residues of cytochrome *c*, and significantly affect the structure and the functional properties of the protein, as the conserved lysine-rich domain around the solvent-exposed heme edge is involved in the interaction with redox partners.

The present data show that divalent anions favor recovery of native-like α-helix structure more effectively than monovalent ions [11] and stabilize a significant population of highly structured macromolecules characterized by M80–Fe(III) coordination and tertiary architecture very close to the native state [29].

This may reflect a different mechanism of binding to the protein: whereas monovalent anions exert an overall ionic strength effect on the macromolecule by nonspecific binding to surface lysine residues, anions carrying a double negative charge may bind to specific sites of the protein.

NMR paramagnetic difference spectroscopy studies have identified three binding sites for polyvalent anions in horse cytochrome *c*. In particular, the locations of these sites are: (a) in the M80-containing loop (this site, which includes K72, K79, and K86, is here indicated as site 0); (b) close to the C-terminal α-helix segment (site 1; see previous section); and (c) at the interface between the C-terminal and N-terminal helices (site 2; see previous section) [18,27]. In this study, the residues supposed to be involved in the interaction with anions were replaced by others occupying the same positions in yeast cytochrome *c*; as mentioned above, horse and yeast cytochrome *c* display very different affinities for anions, despite the close similarity in tertiary architecture [30–33]. For our purposes, this should contribute to the identification of those residues that control and modulate the reaction of the protein with multivalent anions.

The M80-containing loop (a segment formed by residues 70–80) is a highly conserved region of class *c* cytochromes and contains the same amino acid sequence in both horse and yeast iso-1-cytochrome *c* [28]. Therefore, this region provides no discriminatory information on the role played by residues of site 0 in the reaction with anions. By contrast, the side chain segment comprising residues 86–91 (i.e. that containing site 1), which may potentially provide novel and interesting information, is formed by the residues shown in Table 1 (located close or within the C-terminal helix).

In the segment, position 88 is occupied by an acidic residue (E88) in yeast cytochrome *c* and by a basic residue (K88) in horse cytochrome *c*. A recent report identified E62, K88 and R91 as the residues involved in the binding of horse cytochrome *c* to ATP [20]. Therefore, it is possible that residues K88 and R91 modulate protein binding to divalent anions. R91 is an invariant residue in *c* class cytochromes (thus, it is present in both proteins); therefore, we introduced the K88E mutation into horse cytochrome *c*. Support for the hypothesis that the residue located at position 88 influences the protein affinity for divalent anions comes from the fact that it is the first residue of the C-terminal α-helix segment, in both horse and yeast cytochrome *c*; as illustrated in Fig. 7, recovery of the α-helix structure is induced in equine acid-denatured cytochrome *c*, but not in yeast cytochrome *c*, upon addition of sulfate in solution.

Table 1. Amino acid sequence of the horse cyt *c* segment containing site 1 for polyanions.

	86	87	88	89	90	91
Horse	K	K	K	T	E	R
Yeast	K	K	E	K	D	R

Like K88E, the K88E/T89K mutation alters the acid-denatured form, which, with respect to wild-type cytochrome *c*, displays lower absorbance and a red-shift of the CT band associated with an inverse relationship between the absorption bands centered at 497 and 528 nm (Fig. 9A). This suggests that the acid-denatured double mutant possesses less high-spin form than the wild-type protein (confirmed by the intensity of the 620 nm band, also shown in Fig. 9A). However, these differences (also observed for the K13N mutant), do not affect the sulfate–protein interaction significantly. Some effect is instead observed on the dynamics of the anion-linked conformational changes; by analyzing the kinetic scheme previously proposed for the reaction between cytochrome *c* and monovalent anions [18]:

$$\text{HS U-state+sulfate} \underset{\text{(veryfast)}}{\rightarrow} \text{HSA-state} \rightarrow \text{LS}(\text{I}_{\text{HH}})\,\text{A-state} \underset{\text{(fast)}}{\rightarrow} \text{LS}(\text{I}_{\text{HM}})\,\text{A-state} \underset{\text{(slow)}}{} \quad (\textit{Scheme}\ 1)$$

(where HS and LS stand for high- and low-spin, and I_{HH} and I_{HM} indicate the bis-histidine and the His-Met coordinated intermediates) we observe that the sulfate induces a similar kinetic pathway to the refolding reaction of acid-denatured cytochrome *c* (Fig. 8B), even though the rates of the individual steps are significantly faster and the final equilibrium is shifted in favor of the LS (I_{HM}) A-state (that characterized by the native Met80–heme bonding).

In the case of the K88E/T89K mutant, the presence of a relevant amount of LS species already in the acid-denatured form (Fig. 9A) suggests that the double mutation stabilizes the LS (I_{HH}) A-state even in the absence of sulfate. Therefore, the kinetic progress curve of Fig. 9B is expected to refer: (a) for the fast phase, to the sulfate-induced destabilization of the HS acid-denatured form, with further formation of the LS (I_{HH}) A-state; (b) for the slow phase, to formation of the LS native-like (I_{HM}) A-state. Unlike wild-type cytochrome *c*, once the equilibrium is reached, the K88E/T89K mutant displays a higher amount of the LS (I_{HH}) A-state, as indicated by the shape of the absorbance spectrum recorded after 5 s (Fig. 9C), and by the small optical change at 395 nm (Fig. 9B). This is further confirmed by the intensity of the 695 nm

absorption band detected (which is considered to be diagnostic for M–Fe(III)–H coordination [26]; spectra not shown).

Concerning the K13N mutant, the data indicate that the bis-H LS (I_{HH}) A-state stabilization is here more pronounced, this state representing the large majority of macromolecules, both in the absence and in the presence of sulfate (even though the anion shifts the equilibria of Scheme 1 rightwards).

As a whole, it appears that the K88E, K88E/T89K and K13N mutations lead to stabilization, in the absence of sulfate, of the misligated bis-H LS (I_{HH}) A-state (although to a different extent for the last mutant). The addition of sulfate does not induce stabilization of the native-like LS (I_{HM}) A-state, as for wild-type cytochrome *c* (Fig. 9B); however, the energetic alteration of the equilibria of Scheme 1 appears not to affect the characteristics of the binding site for anions.

Polyanions (such as phosphates and sulfates) are known to be powerful stabilizers of structured forms of proteins and are often employed in studies aimed at clarifying aspects of the folding process of proteins [34], including cytochrome *c* [18]. Concerning this last protein, fast kinetic studies established that a compact (I_{HH})-state accumulates during the refolding process, as an off-pathway intermediate [9]. It was thus proposed that progressive accumulation of the misligated state, produced in the nascent phase, prevents rapid protein folding into the native conformation. In other words, cytochrome *c* can be trapped in a misligated form when refolding from the unfolded state. The tertiary conformation of the (I_{HH})-state significantly differs from the native conformation, as bis-H coordination to the heme iron implies that the loop containing H26 and H33 flips to the opposite side of the heme with respect to the location occupied in the native protein, and induces wrong segments of the polypeptide chain to come into contact. The data presented in this article provide a substantial contribution to the clarification of some aspects of the refolding process of cytochrome *c*, in particular the following. (a) Unlike monovalent ions, divalent anions act as strong stabilizers of the native-like (I_{HM})-state of the protein; this not only suggests a different binding mechanism, but also indicates that the divalent anion–protein interaction favors in the macromolecule formation of noncovalent crosslinks and interlocked packing, which are important for stabilization of the native state. Thus, the binding of sulfate to the acid-denatured protein promotes the route towards the native conformation. (b) The mutated residues K13, K88, and T89, all located in segments of the polypeptide containing binding sites for polyanions, appear to play a role in favoring protein folding into the native conformation; the mutants investigated, in fact, all show an enhanced population of the (I_{HH})-state and, with respect to wild-type cytochrome *c*, appear to be less sensitive to sulfate. Furthermore, these residues modulate the conformation of unfolded cytochrome *c*, influencing its spin state and the coordination to the prosthetic group.

Experimental procedures

Horse heart cytochrome *c* (type VI) was purchased from Sigma (St Louis, MO, USA) and used without further purification. High-purity guanidine-HCl was obtained from ICN (Costa Mesa, CA, USA). All the reagents used were of analytical grade.

Construction of horse cytochrome *c* expression system

A version of the horse cytochrome *c* synthetic gene was designed on the basis of the sequence of a previously reported cytochrome *c* synthetic gene [35], and its synthesis was accomplished by Primm srl (Milano, Italy). The synthetic gene was flanked by the *Nco*I and *Bam*HI restriction sites, at the 5′- and 3′-ends, respectively. The pBTRI plasmid was converted to the horse cytochrome *c* expression plasmid by removing the yeast iso-1-cytochrome *c* gene and replacing it with the new synthetic horse cytochrome *c* gene, by using the unique *Nco*I and *Bam*HI sites. The sequence of the expression construct (pHCyc) was confirmed by DNA sequencing (M-Medical, Milano, Italy). Mutagenesis reactions were performed on the pHCyc plasmid in order to introduce the single K88E, T89K or K13N substitution into the horse cytochrome *c* gene. Production of the double mutant K88E/T89K was achieved from the single mutant pHCyc-K88E plasmid, which was used as template in a second round of mutagenesis.

Cell growth and purification of recombinant horse cytochrome *c*

The expression plasmid of horse cytochrome *c* was introduced into *Escherichia coli* JM 109 strain; bacterial expression and purification of the recombinant protein were then conducted as previously described [25]. Briefly, *E. coli* strain JM 109 containing the pBTRI (or the mutated) plasmid was grown at 37 °C, in 2 L of SB medium containing 100 $\mu g \cdot mL^{-1}$ ampicillin to an absorbance of 0.3 at 600 nm. Induction was accomplished by adding isopropyl-β-D-thiogalactopyranoside to a final concentration of 0.75 mM. Cells were then incubated at 37 °C overnight, harvested by centrifugation at 6084 ***g*** (G53 rotor) in a centrifuge, model RC-5B, Sorvall (New Castle, DE, USA), for 10 min, and

frozen at −80 °C. After thawing, the reddish pellets were resuspended in 50 mM Tris/HCl buffer, pH 8.0 [3–4 mL·(g wet cells)$^{-1}$]. Lysozyme (1 mg·mL^{-1}) and DNase (5 μg·mL^{-1}) were then added to the homogenized cells. The suspension was left in ice for 1 h and then sonicated for 1 min, at medium intensity. After centrifugation, the supernatant was dialyzed overnight against 10 mM phosphate buffer (pH 6.2), and loaded onto a CM 52 column (40 mL bed volume) equilibrated with the same buffer. Purification was performed by eluting the protein with one volume of 45 mM phosphate (pH 6.8)/250 mM NaCl. After purification, the recombinant protein (∼ 500 μM) had a purity > 98% (determined by SDS/PAGE analysis and RP-HPLC; not shown), and was stored at −80 °C in 200 μL aliquots.

CD measurements

Measurements were carried out using a Jasco J-710 spectropolarimeter (Tokyo, Japan) equipped with a PC as a data processor. The molar ellipticity, [θ] (deg·cm^2·dmol^{-1}), is expressed on a molar heme basis in the near-UV (270–300 nm) and Soret (380–450 nm) regions, and as mean residue ellipticity in the far-UV region (200–250 nm, mean residue $M_r = 119$).

Electronic absorption measurements

Electronic absorption measurements were carried out at 25 °C using a Jasco V-530 spectrophotometer. An extinction coefficient $\varepsilon_{408} = 106$ mM^{-1}·cm^{-1} was used to determine sample concentration.

Fast kinetics measurements

Kinetic measurements of the effect of sulfate on acid-denatured cytochrome *c* and variants at pH 2.2 were carried out employing a rapid-mixing stopped-flow apparatus SX.18MV (Applied Photophysics Co., Salisbury, UK) with 1 ms dead time, equipped with a diode array for transient spectra collection over the 350–700 nm absorption range.

Acid-denatured Fe(III)–cytochrome *c* (or the investigated variants) was mixed with the salt solution at pH 2.2, and progress curves were followed at different wavelengths. Spectra were then reconstructed by the signal amplitudes at different wavelengths and time intervals.

Kinetic progress curves were fitted according to the following equation:

$$A_{obs} = A_\infty \pm \sum_{i=1}^{i=n} \Delta A_i \cdot \exp^{(-k_i \cdot t)} \quad (1)$$

where A_{obs} is the absorbance at a given wavelength and at a given time interval, A_∞ is the absorbance at longer time intervals (when the reaction is completed), ΔA_i is the absorbance change for phase *I*, k_i is the rate constant for phase *I*, and *t* is time. The '±' sign means that, at different wavelengths, the absorbance may either decrease or increase.

Acknowledgements

This research was funded in part by grants from the Italian MIUR (PRIN 2004 055484).

References

1 Sosnick TR, Mayne L, Hiller R & Englander SW (1994) The barriers in protein folding. *Nat Struct Biol* **1**, 149–156.
2 Sali A, Shakhnovich EI & Karplus M (1994) How does a protein fold? *Nature* **369**, 248–251.
3 Baldwin RL (1995) The nature of protein folding pathways: the classical versus the new view. *J Biomolec NMR* **5**, 103–109.
4 Bai Y, Sosnick TR, Mayne L & Englander SW (1995) Protein folding intermediates: native-state hydrogen exchange. *Science* **269**, 192–197.
5 Ewbank JJ, Creighton TE, Hayer-Hartle MK & Hartle FU (1995) What is the molten globule? *Nature Struct Biol* **2**, 10.
6 Privalov PL (1996) Intermediate states in protein folding. *J Mol Biol* **258**, 707–725.
7 Dill KA & Chan HS (1997) From Levinthal to pathways to funnels. *Nat Struct Biol* **4**, 10–19.
8 Baldwin RL (1997) Competing unfolding pathways. *Nat Struct Biol* **4**, 965–966.
9 Yeh S-R & Rousseau DL (1998) Folding intermediates in cytochrome *c*. *Nat Struct Biol* **5**, 222–228.
10 Jeng MF, Englander SW, Elove GA, Wand AJ & Roder H (1990) Structural description of acid denatured cytochrome *c* by hydrogen exchange and 2D NMR. *Biochemistry* **29**, 10433–10437.
11 Goto Y, Takahashi N & Fink AL (1990) Mechanism of acid-induced folding of proteins. *Biochemistry* **29**, 3480–3488.
12 Goto Y & Nishikiori S (1991) Role of electrostatic repulsions in the acidic molten globule of cytochrome *c*. *J Mol Biol* **222**, 679–686.
13 Jordan T, Eads JC & Spiro TG (1995) Secondary and tertiary structure of the A state of cytochrome *c* from resonance Raman spectroscopy. *Protein Sci* **4**, 716–728.
14 Pletneva EV, Gray HB & Winkler JR (2005) Nature of the cytochrome *c* molten globule. *J Am Chem Soc* **127**, 15370–15371.
15 Kuroda Y, Kidokoro S & Wada A (1992) Thermodynamic characterization of cyt *c* at low pH. *J Mol Biol* **223**, 1139–1153.
16 Marmorino JL, Lehti M & Pielak GJ (1998) Native tertiary structure in an A state. *J Mol Biol* **275**, 379–388.

17 Santucci R, Bongiovanni C, Mei G, Ferri T, Polizio F & Desideri A (2000) Anion size modulates the structure of the A state of cytochrome *c*. *Biochemistry* **39**, 12632–12638.
18 Sinibaldi F, Howes BD, Smulevich G, Ciaccio C, Coletta M & Santucci R (2003) Anion concentration modulates conformation and stability of the molten globule of cytochrome *c*. *J Biol Inorg Chem* **8**, 663–670.
19 Concar DW, Whitford D & Williams JP (1991) The location of the polyphosphate-binding sites on cytochrome *c* measured by NMR paramagnetic difference spectroscopy. *Eur J Biochem* **199**, 569–574.
20 Sinibaldi F, Mei G, Polticelli M, Piro MC, Howes BD, Smulevich G, Santucci R, Ascoli F & Fiorucci L (2005) ATP specifically drives refolding of nonnative conformations of cytochrome *c*. *Protein Sci* **14**, 1049–1058.
21 Battistuzzi G, Borsari M & Sola M (1997) Anion binding to cytochrome c2: implications on protein–ion interactions in class I cytochromes *c*. *Arch Biochem Biophys* **339**, 283–290.
22 Battistuzzi G, Borsari M, Ranieri A & Sola M (2001) Effects of specific anion–protein binding on the alkaline transition of cyt *c*. *Arch Biochem Biophys* **386**, 117–122.
23 Sinibaldi F, Piro MC, Howes BD, Smulevich G, Ascoli F & Santucci R (2003) Rupture of the H-bond linking two omega-loops induces the molten globule state at neutral pH in cytochrome c. *Biochemistry* **42**, 7604–7610.
24 Pielak GJ, Oikawa K, Mauk AG, Smith M & Kay CM (1986) Elimination of the negative Soret Cotton effect of eukaryotic cytochromes *c* by replacement of an invariant phenylalanine residue by site-directed mutagenesis. *J Am Chem Soc* **108**, 2724–2727.
25 Santucci R & Ascoli F (1996) The Soret CD spectrum as a probe for the heme Fe(III)-Met(80) axial bond in horse cytochrome c. *J Inorg Biochem* **68**, 211–214.
26 Stellwagen E & Cass R (1974) Alkaline isomerization of ferricytochrome *c* from *Euglena gracilis*. *Biochem Biophys Res Commun* **60**, 371–375.
27 Pielak GJ, Auld DS, Betz SF, Hilgen-Willis SE & Garcia LL (1996) Nuclear magnetic resonance studies of class I cytochromes *c*. In *Cytochrome C. A Multidisciplinary Approach* (Scott RA & Mauk AG, eds), pp. 203–284. University Science Books, Sausalito, CA.
28 Moore GR & Pettigrew GW (1990) *Cytochromes c. Evolutionary, Structural and Physicochemical Aspects*. Springer-Verlag, Berlin.
29 Maity H, Maity M, Krishna MMG, Mayne L & Englander SW (2005) Protein folding: the stepwise assembly of foldon units. *Proc Natl Acad Sci USA* **102**, 4741–4746.
30 Bushnell GW, Louie GV & Brayer GD (1990) High-resolution three-dimensional structure of horse heart cytochrome *c*. *J Mol Biol* **214**, 585–595.
31 Louie GV & Brayer GD (1990) High resolution refinement of yeast iso-1-cytochrome *c* and comparison with other eukaryotic cytochromes *c*. *J Mol Biol* **214**, 527–555.
32 Banci L, Bertini I, Gray HB, Luchinat C, Reddig T, Rosato A & Turano P (1997) Solution structure of oxidized horse heart cytochrome c. *Biochemistry* **36**, 9867–9877.
33 Banci L, Bertini I, Bren KL, Gray HB, Sompornpisut P & Turano P (1997) Solution structure of oxidized Saccharomyces cerevisiae iso-1-cytochrome c. *Biochemistry* **36**, 8992–9001.
34 Otzen DE & Oliveberg M (1999) Salt-induced detour through compact regions of the protein folding landscape. *Proc Natl Acad Sci USA* **96**, 11746–11751.
35 Patel CN, Lind MC & Pielak G (2001) Characterization of horse cytochrome c expressed in E. coli. *Protein Expr Purif* **22**, 220–224.